On the evolutionary interplay between dispersal and local adaptation in heterogeneous environments

Andrew Berdahl[1,2], Colin J. Torney[1,3], Emmanuel Schertzer[1,4,5] and Simon A. Levin[1]

1. Department of Ecology & Evolutionary Biology, Princeton University, Princeton, NJ, USA
2. Santa Fe Institute, Santa Fe, NM, USA
3. Centre for Mathematics and the Environment, University of Exeter, Penryn Campus, Cornwall, UK
4. Laboratoire de Probabilités et Modèles Aléatoires des Universités Pierre et Marie Curie et Denis Diderot, Paris, France
5. Collège de France, Center for Interdisciplinary Research in Biology CNRS UMR 7241, Paris, France

Email addresses:

berdahl@gmail.com (Andrew Berdahl)

c.j.torney@exeter.ac.uk (Colin J. Torney)

emmanuel.schertzer@gmail.com (Emmanuel Schertzer)

slevin@princeton.edu (Simon A. Levin)

Running title:

Joint evolution of dispersal and local adaptation

Key words:

Joint evolution, specialization, adaptive radiation, evolutionary branching, meta-population, dimorphic populations

Counts:

Words: 7441

Tables: 1

Figures: 5 (1 and 3-5 use color)

List of elements:

Main text (Manuscript.pdf)

Figures 1-5 (Figure1.pdf, Figure2.pdf ... Figure5.pdf)

Appendices A-G: (Supplementary.pdf)

Submitted to *Evolution*.

Abstract

Dispersal, whether in the form of a dandelion seed drifting on the breeze, or a salmon migrating upstream to breed in a non-natal stream, transports genes between locations. At these locations, local adaptation modifies the gene frequencies so their carriers are better suited to particular conditions, be those of newly disturbed soil or a quiet river pool. Both dispersal and local adaptation are major drivers of population structure; however, in general, their respective roles are not independent and the two may often be at odds with one another evolutionarily, each one exhibiting negative feedback on the evolution of the other. Here we investigate their joint evolution within a simple discrete-time, metapopulation model. Depending on environmental conditions, their evolutionary interplay leads to either a monomorphic population of highly dispersing generalists or a rarely dispersing, locally adapted, polymorphic population, each adapted to a particular habitat type. A critical value of environmental heterogeneity divides these two selection regimes and the nature of the transition between them is determined by the level of kin competition. When kin competition is low, at the transition we observe discontinuities, bistability and hysteresis in the evolved strategies; however, when high, kin competition moderates the evolutionary feedback and the transition is smooth.

1. INTRODUCTION

Dispersal is a fundamental process in ecology that is significant over many different scales of organization. At the scale of the individual, it determines survival rates and offspring viability. At the meta-population scale it modulates genetic diversity and couples the dynamics of spatially distinct populations, while at the ecosystem scale dispersal processes determine connectivity and nutrient transport. For these reasons there has been much theoretical and empirical work in this area (Colbert et al. (2001); Johnson and Gaines (1990); Levin et al. (2003); Ronce (2007)). It has been shown that dispersal reduces kin competition (Hamilton and May, 1977; Leturque and Rousset, 2002; Perrin and Mazalov, 2000) and inbreeding depression (Bengtsson, 1978; Gandon, 1999; Pusey and Wolf, 1996). It is thought that spatial-temporal variation in the environment can select for, or against, dispersal (Duputié and Massol, 2013). On one hand, environmental heterogeneity may reduce dispersal by increasing the risk of ending up in unsuitable habitat (Hastings, 1983; Holt, 1985); but on the other, increased dispersal could allow organisms to hedge bets over environmental fluctuations (Blanquart and Gandon, 2011; Levin et al., 1984).

Simple models have demonstrated how dispersal can be selected for in stable environments, even when the associated risks are extremely high (Comins et al., 1980; Hamilton and May, 1977). In their classic paper, Hamilton and May (1977) collapsed the costs of dispersal into a single parameter. They showed that when the number of offspring that parents produce is high at least half of all offspring should be dispersed, regardless of the potential costs. However, it is insightful to categorize the cost of dispersal into two components: the risk associated with movement, and the risk of landing in a habitat that is unsuitable. Hamilton and May's model is well suited to address the first cost, but for the second to fit into their framework one must assume the environment is binary, composed of regions where the probability to survive is either 0 or 1. This scenario cannot capture the more continuous variation found in nature; and it neglects the possibility of explicit local adaptation to a particular habitat.

The relative quality of a habitat is a subjective measure, specific to each species or phenotype. In general, there are no 'good' or 'bad' habitats, only conditions that are better or worse for a specific type of organism. Much of the biodiversity we observe, both between and within species, is due to selection acting differently in various environments, causing specialization for habitats with particular conditions and thus local adaptation. For reviews of this field see, for example, Coyne et al. (2004); Futuyma and Moreno (1988); Schluter (2000); Turelli et al. (2001).

Both dispersal and local adaptation play fundamental roles in shaping population structure and, in general, it is expected that natural selection will result in a negative correlation between the traits associated with each of these factors. Dispersal will impede diversification of local adaptation traits by inducing gene flow between different habitat types, or by increasing the heterogeneity in the range of environments a lineage experiences over multiple generations (Day, 2001; Doebeli and Dieckmann, 2003; North et al., 2011). Conversely, in a heterogeneous environment,

local adaptation to a particular habitat type will raise the risk associated with dispersal by increasing the probability of arriving at an unsuitable habitat (Comins et al., 1980; Hastings, 1983; Massol and Cheptou, 2011). Despite their evolutionary consequences being deeply intertwined, few studies have considered the joint evolution of dispersal and local adaptation, aside for a few notable and interesting exceptions: Kisdi (2002); Heinz et al. (2009) and Nurmi and Parvinen (2011).

In a seminal study of the joint evolution of dispersal and specialization Kisdi (2002) modeled a population that could disperse between two patches and become specialized to either. Temporal fluctuation in habitat quality induced dispersal while long-term average environmental properties provided incentives for specialization. Various stable evolutionary strategies emerged depending on the difference between the two patches and the initial conditions, leading to hysteresis in the evolved strategies for dispersal and specialization.

Later, using spatially explicit simulations, Heinz et al. (2009) found that slight environmental gradients led to the evolution of long range dispersal and a lack of specialization while steep environmental gradients led to reduced dispersal and specialization to local condition. They observed a sharp boundary between these two regimes and posited that this transition was due to feedback between specialization and reduced dispersal.

Nurmi and Parvinen (2011) modeled the evolution of dispersal between many, non-spatially explicit, patches and specialization onto either of two resources available in different ratios on different patches. Local extinction events select for dispersal while increased mortality during dispersal selected against it. Investigating the joint evolution of dispersal and specialization led to outcomes not predicted by the evolution of either trait singly, most notably a co-existence of high and low dispersers.

Billiard and Lenormand (2005) and Blanquart and Gandon (2014) used genetically explicit models to explore the evolution of dispersal probability under the influence of local adaptation. Both models assume that dispersal and local adaptation are encoded by two genes on a single chromosome. Dispersal probability can evolve a continuous range of values while specialization adopts one of two values and is under spatially variable selection in a two-patch (Billiard and Lenormand, 2005) or metapopulation (Blanquart and Gandon, 2014) model. Depending whether or not a polymorphism at the local adaptation locus is protected, the evolved level of dispersal is high or low. As in Kisdi (2002), for certain parameter values both high and low dispersal states are stable depending on the initial conditions.

Together these studies demonstrate the importance of considering the joint evolution of dispersal and local adaptation. In this work, we have created a spatially implicit metapopulation model in which the ecological characteristics of available breeding sites are drawn from a continuous distribution of site types, reflecting the continuous clines found in nature. Individuals evolve a probability to disperse and to adapt to different site types. In line with the distribution

of site types, individuals can evolve a continuous and unbounded range of ecological characters, allowing for arbitrary specialization and branching patterns to evolve. In contrast to most models described above, in our model kin competition, rather than local extinction events or temporal variation in habitat quality, selects for dispersal. Environmental heterogeneity selects against dispersal, by increasing the risk of landing on unsuitable habitat, but also selects for local adaptation. Within our model, we are able to continuously, and independently, vary the level of both kin competition and environmental heterogeneity.

Our findings demonstrate that the joint evolution of dispersal and local adaptation can lead to qualitatively distinct stable strategies as environmental heterogeneity is varied and that the level of kin competition determines the nature of the transition between those population-level patterns. Analysis of our simple model illustrates how the interaction between two traits can lead to rich phenomena such as discontinuous phase transitions and hysteresis effects, and how small fluctuations of environmental conditions can trigger drastic changes in the evolutionary outcome.

In this study, we propose semi-analytical methods to explain quantitatively the mechanisms behind the abrupt transition in level of dispersal and degree of specialization observed in similar models (Heinz et al., 2009). Employing multi-dimensional adaptive dynamics (Geritz et al., 1998; Leimar, 2005; Metz et al., 1992), we first show that branching occurs at an evolutionary singular strategy. In a multidimensional trait space, this branching leads to highly nonlinear responses to environmental perturbations. As in Ito and Dieckmann (2007), the joint evolution of multiple traits creates feedbacks and discontinuous transitions in evolutionarily stable strategies (ESS) (Maynard Smith and Price, 1973). Understanding these processes requires the study of the interactions between multiple sub-populations, and the combinations (Cohen and Levin, 1991; Ludwig and Levin, 1991) of their traits.

We hope that our approach will be relevant in a more general setting, and will be useful when identifying and explaining sudden regime changes in multi-dimensional evolutionary systems. For instance, this framework may be applicable to the joint evolution of dispersal and a wide array of other traits, including co-operation (Le Galliard et al., 2005; Parvinen, 2013), seed dormancy (Cohen and Levin, 1987; Olivieri, 2001; Venable and Brown, 1988), reproductive effort (Crowley and McLetchie, 2002; Ronce et al., 2000), sex ratios (Leturque and Rousset, 2003), kin recognition (Lehmann and Perrin, 2003), inbreeding load (Guillaume and Perrin, 2006), mating strategy (Ravigné et al., 2006), habitat niche width (Chaianunporn and Hovestadt, 2012) and age at death (Dytham and Travis, 2006).

2. MODEL

We consider a population of individuals characterized by a probability to disperse, v, and an ecological type, x. These agents inhabit an array of L discrete sites ($L >> 1$) without explicit spatial locations. Each site, i, in the array can accommodate up to K breeding adults and is assigned an ecological character, z_i, that remains fixed over time and

is drawn from a normal distribution,

$$p(z) = \frac{1}{\sqrt{2\pi}\sigma_z} \exp\left[-\frac{z^2}{2\sigma_z^2}\right]. \quad (1)$$

Every discrete generation has two stages. During the first stage adults produce m offspring, that inherit the adult's ecological type, x, and probability to disperse, v, with some small mutation (see Numerical Simulations section for details). The adult then perishes. Next each juvenile disperses to a randomly selected site with probability v or returns to its natal site with probability, $1 - v$. If there are greater than K juveniles on a given site they compete for space, and a random set of K survive After this competition, juveniles mature into adults and become the parents of the next generation.

The number of offspring a parent leaves behind, m, is a function of the difference between the parent's ecological type and the ecological character of the site at which it breeds. This is given by,

$$m(x, z) = m_o \exp\left[-\frac{(x - z)^2}{2\sigma_m^2}\right], \quad (2)$$

where m_o is the maximum number of offspring and σ_m determines the width of this bell-shaped function, i.e. the tolerance of individuals to variation in habitat. Our results are independent of m_o provided that $m_o >> K$, which leads to all sites being saturated.

In our model the heterogeneity of the environment is determined by the width of the distribution of site types (Equation 1). The wider this distribution is, the greater will be the range of site types a dispersing individual could encounter. This scale matters only in relation to the width of the fecundity curve, or the plasticity of the organisms, defined by Equation 2. Thus we define a rescaled environmental heterogeneity parameter as $\sigma = \sigma_z/\sigma_m$ and nondimensionalize all ecological characteristics by σ_m in the results that follow.

3. NUMERICAL SIMULATIONS

We performed evolutionary simulations of our model. Unless noted otherwise, all simulations were initialized with monomorphic populations having probability to disperse, $v = 1$, and ecological character, $x = 0$. During the simulations, each offspring inherited the values of v and x from its parent plus small independent mutations, consistent with a continuum-of-alleles genetic model. However, it was not meant to reflect the actual evolutionary dynamics of any organisms, but rather to allow the dynamics to take the system to an ESS. Mutations were drawn from a normal distribution centred at zero with a variance of 10^{-8} for dispersal probability and 2.5×10^{-7} for ecological character. For the probability to disperse, if the mutation put the trait below 0 or above 1 the trait was reset to 0 or 1 respectively. No restrictions were placed on the value of x.

Figure 1 shows the evolution of dispersal and local adaptation over time. Depending on the environmental heterogeneity, σ, and the carrying capacity, K, the distribution of evolved ecological characters was either a narrow monomorphic peak centered at $x = 0$ (lower left panels of Figure 1), or a pattern of discrete regularly spaced peaks in x-space (lower right panels of Figure 1). We interpret a monomorphic population having $x = 0$ as a population of generalists, as they have evolved to the mean of the distribution of site types. Conversely, a population of discrete x-types, many far ($> \sigma_m$) from the average value of z, we interpret as a population of specialists. These populations have undergone evolutionary branching and are locally adapted to specific site types.

We observe a negative correlation between dispersal rate and $|x|$ in some simulations, especially for high K and when environmental heterogeneity is just above the minimum σ needed for branching to occur (Appendix Figures E.3 & G.6). However, the slope of the trend is shallow, and often there is no, or even a positive, relationship between v and $|x|$ (Appendix Figures E.1-3). In general, the range of v across the branches is so narrow that it is well characterized by the mean (see Appendix Figure G.6, for the distribution over a range of parameter values).

It is interesting to note that even within an environment that will select for generalists, branching can initially occur if dispersal probability is 'artificially' low. We see this in the bottom left panel of Figure 1, because the simulation is started with $v = 0$ branching initially occurs, but the generalist strategy supplants it once dispersal rises. Similarly, in the middle right panel, even though the environmental heterogeneity is appropriate to select for specialists, this branching does not occur until the probability to disperse falls below this threshold. Thus from the point of view of one trait, the state of the other trait is part of the selective environment. Overall, comparing the left and right sides of Figure 1 we can see that a small change in environmental heterogeneity can produce a significant quantitative change in v and a dramatic qualitative change in the distribution of x. This dramatic change is due to the joint evolution of the two traits and the feedback between them. and is mediated by the level of kin competition, K.

In Figure 2 we show the mean evolved value of dispersal, $\tilde{v}$, and the distribution of the ecological characteristic, x. Both Figure 1 and Figure 2 demonstrate that there exists a threshold level of dispersal, v_c, below which individuals will tend to specialize and branching in x will occur. Above this boundary the dynamics will select for a monomorphic population of generalists having $x = 0$ (the average of the ecological character across the environment). The top panels of Figure 2 show this transition in v-σ space. For each K there is a unique threshold level of environmental heterogeneity below which specialization is impossible.

To understand these numerical results we next examine the behaviour of a monomorphic, evolving population.

4. ADAPTIVE DYNAMICS AND ESS CALCULATIONS

We consider a monomorphic resident population with probability to disperse, v, and ecological character, x, and a rare invader characterized by v' and x'. A required condition for this phenotype to successfully invade the population and replace the resident is that the expected growth rate of the mutant, when initially rare, is positive. Following Metz and Gyllenberg (2001) and Ajar (2003) (but also see Chesson (1984)) we define the metapopulation reproduction ratio, R_m, as the expected number of dispersers produced by a single mutant starting in the disperser pool[1]. Here we will use R_m to show that the singular strategy for local adaptation is, as one might expect, the most common (and average) environmental type, while the value for dispersal is determined by a balance between kin competition and environmental heterogeneity. This technique should apply for arbitrary distributions of site types, $p(z)$, and is thus not limited to the Gaussian distribution (Equation 1) we have used in this study.

Assuming $m_o >> K$, and thus every site holds greater than K individuals before competition, the probability that a dispersing mutant will survive to breed, given it has landed on a site of type z is

$$\frac{1}{v\bar{m}(x) + (1-v)m(x,z)} \tag{3}$$

where $\bar{m}(x)$ is the expected number of offspring produced by the resident population per site, when the invader is rare, and can be calculated as

$$\begin{aligned} \bar{m}(x) &= \int_{-\infty}^{\infty} p(z)m(x,z)dz \\ &= \frac{m_o}{\sqrt{1+\sigma^2}} \exp\left[-\frac{x^2}{2(1+\sigma^2)}\right]. \end{aligned} \tag{4}$$

Given that an invader has gained a foothold on a site, its lineage will persist there for some finite time before losing the site. Over this persistence time it will produce some total number of offspring, a fraction v' of which will disperse. We will define the expected number of dispersing offspring an invader lineage will produce at a site of type z before losing that site to be $M_{v,x,v',x'}(z)$, but for convenience refer to it from here forward as $M(z)$. This quantity represents the total number of offspring produced from first occupation until no descendants of the original mutant are present. Finding $M(z)$ involves the solution to a set of K equations, however, following Ajar (2003) we are able to find to find its derivative at the singular strategy. In Appendix A, we extend the method of Ajar (2003) to heterogeneous environments such as the one at hand.

[1]Note that Ajar (2003) uses a slightly different formulation "...overall [expected] production of successful emigrants from a patch, descended from a single mutant immigrant in this patch", but both verbal descriptions lead to the same mathematical expression.

The expected contribution to the mutant disperser pool by each mutant disperser when rare, is then given by the product of the probability to capture a site (Equation 3) and the expected number of dispersers produced during its lineage's tenure on that site ($M(z)$), averaged over all possible site types.

$$R_m = \int_{-\infty}^{\infty} \frac{p(z)M(z)}{v\bar{m}(x) + (1-v)m(x,z)} dz \tag{5}$$

The logarithm of the metapopulation reproduction ratio is sign equivalent to the standard fitness measure, the invasion exponent; thus the derivatives of R_m with respect to the mutant variables will define the selection gradient, $\mathbf{S}$. To solve for the singular strategy, (v^*, x^*), we must find where the selection gradient is equal to zero. When this condition is satisfied, the resident will occupy an extremum of the fitness landscape and hence this point will potentially be a convergence stable and/or evolutionarily stable strategy. The selection gradient is given by

$$\mathbf{S} = \left[\begin{array}{c} \frac{\partial R_m}{\partial v'} \\ \frac{\partial R_m}{\partial x'} \end{array} \right] \Bigg|_{\substack{v'=v \\ x'=x}} . \tag{6}$$

As we demonstrate in Appendix A, the singular strategy for the ecological character is $x^* = 0$, while the singular dispersal strategy, v^*, is given by the solution to

$$\mathrm{Var}\left[m(0,z)\right] = \int_{-\infty}^{\infty} m(0,z)^2 (1 - d^*(z)) F^*(z) p(z) dz, \tag{7}$$

where $F(z)$ is a measure of population structure, specifically, the probability that two individuals randomly selected from the same site have a common ancestor at that site (see appendix, Equation A.17) and $d(z)$ is the probability of a resident immigrant being selected to breed at a site of type z (see appendix, Equation A.9). The *s indicate that they are evaluated at the singular strategy, $(v^*, 0)$. The solution to Equation 7 is is plotted for $K = 1, 2$ & 8 in Figure 2.

The Jacobian matrix of the selection gradient, $\mathbf{S}$, can be used to determine the convergence stability of this singular strategy, while the Hessian matrix of the metapopulation reproductive ratio, R_m, can be used to determine its local evolutionary stability (uninvadability) (Geritz et al., 1998; Leimar, 2005) - see Appendices B & C for details. For all values of K and σ the Jacobian matrix evaluated at the singular strategy ($v = v^*, x = 0$) is negative definite (shown in Appendix B), indicating this strategy is convergence stable and the evolutionary dynamics will converge towards it (Geritz et al., 1998; Leimar, 2005). If this singular strategy is also locally uninvadable (negative definite Hessian matrix) it is an ESS (Maynard Smith and Price, 1973). The definiteness of the Hessian matrix is dependent on K and σ, thus the ($v = v^*, x = 0$) is not always an ESS (see Figure 2 and Appendix C).

5. DISCONTINUITIES AND HYSTERESIS IN EVOLVED STRATEGIES

5.1. Numerically observed transitions

As the degree of environmental heterogeneity is increased from zero, the evolved dispersal strategy, $\tilde{v}$, matches the singular strategy for the monomorphic population, v^*. When the critical value of environmental heterogeneity, σ_c, is reached the convergence stable strategy is no longer evolutionarily stable and the population branches. After this occurs, the evolutionary attractor for the level of dispersal is no longer given by the monomorphic singular strategy defined by Eqn. 7, i.e. $\tilde{v} \neq v^*$.

In the lower panel of Figure 2, we plot the evolved distribution of x as a function of environmental heterogeneity, σ. The distribution turns from uni- to multi-modal as the v^* curve crosses the generalist-specialist boundary. For large K there is a discontinuity in both the variance in the distribution of x, and the stable level of dispersal, $\tilde{v}$. This is caused by the interplay between local adaptation and dispersal. Once the critical level of environmental heterogeneity is reached, disruptive selection causes branching in the ecological characteristic, x, and we are left with a multi-peaked distribution in x, with each sub-population adapted to a different environmental character (lower panels of Figure 2). This local adaptation feeds back on the level of dispersal, selecting for lower dispersal rates, which in turn feeds back into the selection for further local adaptation.

Returning briefly to the top right panel of Figure 1, we can see this feedback play out over time. Because selection is increasingly relaxed as v approaches the singular strategy the blue curve (population starting with $v = 1$) is concave-up during this time period. However, once v falls below v_c branching occurs and this local adaptation causes renewed selection for lower dispersal, which is apparent in the negative concavity of the blue v curve as the population accelerates downward in v due to this feedback.

5.2. A geometric explanation for discontinuous transitions

In Section 4, we studied the evolutionary gradient for a monomorphic population and used nullclines of this gradient to identify singular strategies and their stability. In particular, we showed the existence of a critical value σ_c above which branching occurs, transitioning from a monomorphic (generalist) to a polymorphic (specialist) population. In this section, in order to explain the nature of the transition (and the observed abrupt change for large enough K), we consider a population that has undergone symmetric branching in the ecological character trait, x. In general we would have to consider a mutant arising in a dimorphic population of resident individuals of type (x_1, v_1) and (x_2, v_2). However, to make this situation more tractable we suppose half of the population has ecological character x, and the other half $-x$, but all have the same dispersal probability, v. We note that this is indeed what we observe in numeric simulations, for any K, immediately after the first branching occurs from the monomorphic singular strategy, $(v^*, 0)$

(see for example Figure 1). As we shall see, reducing the dimension of the problem (from 4 to 2) will allow us to give a geometric interpretation of the observed discontinuity at the transition from a monomorphic (generalist) to a polymorphic (specialist) population, for large enough K.

We plot the nullclines of the evolutionary gradient for each coordinate for the dimorphic, symmetric population in v-x space, as an illustrative schematic in Figure 3 and also confirm this picture using simulation data (Figure F.4). In these figures, the red curves are the nullclines for the x-coordinate; in biological terms, this is the evolved branch separation of ecological character for the dimorphic population when all individuals have a fixed dispersal probability, v. The red curve can be decomposed into two components. For a high enough value of the dispersal probability, v, the dimorphic equilibrium is the monomorphic (degenerate dimorphic) equilibrium $x = -x = 0$. If successive generations visit many different sites, the evolutionary dynamics drive the population to a generalist strategy. When dispersal is lowered below a critical value of v_c, the population experiences branching and the convergence dimorphic equilibrium is at $(x, -x)$, with $(x \neq 0)$. This point may be stable (locally uninvadable) or unstable (locally invadeable) and result in further branching (discussed later).

The blue curves of Figures 3 & F.4 are the nullclines for the v-coordinate; they indicate evolved dispersal probability, v, as a function of a fixed value of the ecological character, $\pm x$, of the dimorphic population. As intuition suggests, the v-curve attains its maximum value at $x = 0$ (generalist population). This is consistent with the idea that dispersing is more risky when the site type one is adapted to is more rare.

Where these curves intersect are singular strategies, which may be stable (solid black circles), convergence stable but evolutionary unstable (dashed black circles) or convergence unstable (black triangles). The relative position of the peak of the blue curve and the fork of the red curve depends on the value of the heterogeneity σ. As σ increases the peak of the blue curve (v^*) descends while the fork of the red curve (v_c) increases. At low environmental heterogeneity ($\sigma < \sigma_c$), the blue curve intersects the stable, degenerate, section of the red vertical line (blue line above the red fork, left column of Figure 3). This intersection point coincides with the stable, generalist, monomorphic equilibrium described in Section 4. Conversely, for $\sigma > \sigma_c$, the peak of the blue curve intersects the unstable section of the red vertical line (blue curve below the red fork, right column of Figure 3). This point coincides with the the evolutionarily unstable singular (generalist) strategy. Finally, the critical environmental heterogeneity ($\sigma = \sigma_c$) is characterized by a tangency property between the peak of the blue curve and the red fork (middle column of Figure 3).

Figure 3 demonstrates how the relative curvature of the $v^*(\pm x)$ and $\pm x^*(v)$ curves when $\sigma = \sigma_c$ determines whether or not there will be a direction of instability along the plane tangent to the symmetric dimorphic manifold. Such an instability results in a discontinuity in the ESS level of dispersal, and the variance in ecological character, as a function of environmental heterogeneity, σ. The top and bottom rows of panels in Figure 3 correspond to the two scenarios

described below:

(i) Given that we have restricted the evolutionary dynamics to a symmetric (in x) dimorphic population, if the concavity of $v^*(\pm x)$ (blue) is greater than that of $\pm x^*(v)$ (red) at σ_c, as in the top row of Figure 3, then this guarantees that the symmetric manifold defines a direction of stability for the system. In this case, as σ increases, the $(v^*, 0)$ strategy becomes unstable and creates two stable (along the symmetric sub-manifold) strategies infinitesimally close and there will be a kink, but no discontinuity, in the evolved probability to disperse, $\tilde{v}$, and the variance in x will transition continuously from zero to positive values (upper right panel of Figure 3). We note that this two-dimensional picture does not guarantee actual stability of the symmetric dimorphism, only its stability if the system is restricted to be symmetric, however, simulations of the full model suggest that the symmetric dimorphism is stable for low K (Figure 2).

(ii) If, however, the concavities are reversed (lower row of panels), when $\sigma = \sigma_c$ the $(v^*, 0)$ strategy is unstable (lower middle panel) and $\tilde{v}$ makes a discrete jump to the symmetric pair of lower intersection points, and thus there is a discontinuity in $\tilde{v}$ at σ_c when crossing from above. This lower singular strategy may be an ESS or could be convergence, but not evolutionarily, stable and further branching in x could occur, in which case the dimorphic plots in Figure 3 will no longer apply (discussed in Section 5.2.1).

We confirmed the theoretical picture presented in Figure 3 by simulating the dimorphic populations described above to find the fitness gradient in x-v space (see Appendix D for details). Numerically, we observe relative curvatures matching, qualitatively, the top row of Figure 3 for $K = 1$ & 2 and matching the bottom row for $K = 8$ (Figure F.4). This indeed matches the presence and absence of discontinuities for those values of kin competition in Figure 2. At the transition ($\sigma = \sigma_c$) the concavity of both the red, $x^*(v)$, and blue, $v^*(x)$, curves increase as a function of K. The $x^*(v)$ curve does so because σ_c decreases as a function of K, so there is less incentive to specialize further at the branching point. The $v^*(x)$ curve is more concave at higher values of K because with lower kin competition dispersal is more free to fall off away from $x = 0$ since it is not propped up by a drive to disperse to avoid competition with kin locally (Comins et al., 1980). The ranks of the concavities are able to switch because the concavity of the dispersal curve varies much more rapidly with K than the x curve does. Thus it is the change in kin competition that determines whether or not there will be a discontinuity in $\tilde{v}$ and the generalist-specialist transition.

5.2.1. Branching Cascade.

If the monomorphic stationary point $(v^*, 0)$ is unstable at $\sigma = \sigma_c$ (scenario (ii) from the list in the preceding section), two possibilities arise. Either, the population stabilizes to a dimorphic stable equilibrium (indicated by the solid circles in the lower, middle panel of Figure 3), or further branching events occur. The subsequent branching in

the lower right panels of Figure 1 demonstrate that for low kin competition ($K = 8$) this equilibrium is unstable in the x coordinate. Further we note that the monomorphic singular strategy $(v^*, 0)$ is in the basin of attraction of this symmetric, dimorphic, point. (See, for example, the middle right panel of Figure 1.) The population first evolves to the singular strategy $(v^*, 0)$, then, if $\sigma > \sigma_c$, this monomorphic singular strategy is unstable and disruptive selection causes branching before directional selection drives the population to a symmetric (in x) evolutionary singular dimorphism. Upon reaching this point, directional selection ceases and disruptive selection in the x-direction arises, leading to further branching events in the evolutionary tree. This is indeed what we observe for $K = 8$ (shown in Figures 2 & G.6-9), here the population goes from being monomorphic to consisting of five sub-populations as the environmental heterogeneity passes σ_c. Contrasting this sudden shift from one to many branches as environmental heterogeneity passes a critical level, with the more continuous shift from one to two to three branches exhibited by a similar model in which dispersal is fixed (Geritz et al., 1998), implicates the role of feedback due to the joint evolution of dispersal and local adaptation in the present model.

5.3. Hysteresis in the response to changing environmental variability

Another interesting feature of Figure 3 is the presence of two alternate stable strategies in the lower left panel, ($\tilde{v}_a$,0) and ($\tilde{v}_b$,$\pm x$). This suggests that for large K, and environmental heterogeneity less than, but close enough to, σ_c we should expect alternative stable states, one of highly dispersing generalists and the other of a pair of relatively rarely dispersing specialist lines (or the polymorphic population left after a branching cascade from this initial pair), depending on initial conditions. Such bistability is often encountered around transitions from mono to polymorphic ESSs (Geritz et al., 1999). In Figure 4, we plot the ESS dispersal probability from Figure 3 as a function of environmental heterogeneity and carrying capacity – solid, dashed and dotted lines in right hand panels of Figure 4 correspond to stable (solid black circles), convergence stable but evolutionary unstable (dashed black circles) or convergence unstable (black triangles) intersections in Figure 3 respectively. When the concavity of the blue curves is greater than that of the red curve, we observe a destabilization of the upper curve and thus a sudden jump to the lower curve, at the point σ_c (bottom right panel); the fold disappears when the concavities are reversed (top right panel). The cusp-like nature of the $\tilde{v}$ curve introduces two discontinuities around a region of bistability, leading to a hysteresis loop in both environmental parameters: σ and K.

This bistability is apparent in Figure 5, which shows results from simulations with environmental heterogeneity around σ_c for various initial configurations of individual trait values. In contrast to Figure 1, the left panels of Figure 5 shows a value of σ for which the outcome of the evolutionary dynamics is dependent on the initial state of the system. The full range of environmental heterogeneity leading to bistability is highlighted in yellow in the right panel of Figure 5. Note that the value of σ at which the blue and red curves become tangent in the bottom left panel of

Figure F.4 corresponds to the left boundary of this region of bistability shown in yellow. Here the blue crosses depict simulations seeded with a population all having full dispersal and no specialization ($v = 1$, $x = 0$), as in Figure 2, while red circles represent simulations starting with non-dispersing, locally adapted populations ($v = 0$, $x = z$). As predicted, the region of bistability, bounded by discontinuities in the evolved dispersal probability, $\tilde{v}$, and variance of x creates a potential hysteresis loop for the evolutionary dynamics. For $K = 8$ (shown in Figure 5), moving from high to low environmental heterogeneity (right to left), a population of specialists will encounter an abrupt jump upwards in their evolved dispersal probability, $\tilde{v}$, and a collapse of the variance in x around $\sigma = 0.8$. However, if environmental heterogeneity were to then smoothly increase that population would not return to the specialized state until σ was around 0.9.

5.4. Asymmetric environments

Symmetric environmental distributions represent a special case, which due to their tractability are often useful for gaining intuition. In general, the picture presented in Figure 3 can be qualitatively different. Specifically, for non-symmetric distributions, the evolved trait values of a dimorphic population (red branches in Figure 3) do not converge on the monomorphic singular strategy. Rather only one of the dimorphic branches connects continuously to the monomorphic strategy while the other appears some finite distance away (Geritz et al., 1999).

The analysis in Section 5 relies on the symmetry of distribution of site types. To reveal which results are general and which are specific to the symmetric case we explore numerically the behaviour of our model in environments with varying degrees of asymmetry (see Appendix E). Strictly speaking, the asymmetry in $p(z)$ creates a discontinuity in the evolved values of v and x for all values of K. However, for moderate levels of asymmetry the discontinuities at low K are too small to be seen and thus the results are very similar to the symmetric case (Figure F.4). For all distributions of z, regardless of symmetry, for high K the population transitions from one to many branches in x as σ passed σ_c, while for low K the number of branches in x transitions more smoothly from 1 to 2 to 3, and so on. Preserved, even for highly asymmetric distributions, is the result that multiple branching in x, immediately after the singular strategy becomes unstable (ie. when $\sigma = \sigma_c + \epsilon$), is only observed for high K.

This is because at low K high kin competition provides additional evolutionary force towards increased dispersal; however, when kin competition is lower specialization has a greater relative role in shaping dispersal, so the positive feedback between increased specialization and decreased dispersal is more free to play out. Thus, in general discontinuities and hysteresis may always be present in asymmetric environments, however, the size of the discontinuity will be governed by the amount of kin competition, with less kin competition (higher K) leading to larger discontinuities and regions of hysteresis.

6. DISCUSSION

Dispersal and local adaptation are major drivers of ecological patterns and for that reason they have both been the subject of many studies. However, the interplay between dispersal and local adaptation has the potential to shape the evolutionary process in unforeseen ways. The purpose of this work is to explore their joint evolution in general heterogeneous environments.

To investigate the specific case of joint evolution at hand, we have modified one of the simplest models of dispersal, that of Hamilton and May (1977), by adding the potential for individuals to adapt to a general, permanent and heterogeneous feature of the landscape and by increasing the local carrying capacity of a patch beyond one, to allow us to investigate the role of variable kin competition. In this simple model, increased environmental heterogeneity increases local adaptation, while local carrying capacity dictates the level of kin competition, and thus modulates the pressure to disperse.

We found the evolutionary gradient in monomorphic strategy space by considering the reproductive success of a lineage during its persistence time at a single site (Ajar, 2003; Metz and Gyllenberg, 2001). Using nullclines in this gradient allowed us to calculate the singular strategy for dispersal as a function of environmental heterogeneity and carrying capacity, as well as predict whether natural selection would favor a homogeneous generalist population, or lead to evolutionary branching and locally adapted specialists. Next, we studied the evolutionary dynamics in a larger strategy space (i.e., the space of symmetric and dimorphic populations), and we showed how the geometry of the nullclines in the evolutionary gradient could partially predict the nature of the transition between these population-level states of the system. Certain relative concavities of the nullclines can lead to discontinuities in evolutionary outcomes, branching cascades, bistability and hysteresis. This analysis relied on the symmetric environmental distribution of site types, however, this special symmetric case provides insight and guides intuition for more general cases, which we have shown exhibit similar dynamics.

For a given value of environmental heterogeneity and carrying capacity, a threshold value of dispersal, v_c, marked the boundary between two selection regimes. When environmental heterogeneity was low, such that the singular strategy for dispersal, v^*, was greater than v_c, selection was for generalists and v^* was the ESS (ie. $\tilde{v} = v^*$). However, above a critical value of environmental heterogeneity v^* fell below v_c and the dynamics shifted to selection for specialization (Svardal et al., 2015). Varying the level of kin competition, K, had several effects on the evolutionary outcome. As kin competition was reduced (K is increased) the critical level of environmental heterogeneity, above which branching occurs, decreased. If kin competition was too high (small K) we did not see a discontinuity in the ESS level of dispersal, $\tilde{v}$, as the threshold level of environmental heterogeneity was crossed.

By examining the dynamics close to the transition, we can understand the nature of the discontinuity in the evolu-

tionary stable strategies. Increased pressure to specialize due to an effective increase in environmental heterogeneity makes dispersal less favorable. The associated reduction of dispersal then leads to selection for further local adaptation, creating a positive feedback loop between reduced dispersal and increased specialization (Heinz et al., 2009). When kin competition is low (high K) there is little additional pressure to disperse to avoid competing with kin and thus this feedback loop is relatively unconstrained. In this scenario, the positive feedback induces a discontinuity in the ESS level of dispersal which creates the spontaneous transition from selection for generalists to selection for specialists. Close to this transition the evolutionary dynamics exhibit hysteresis, and the population can evolve to the highly dispersing generalist, or the rarely dispersing specialist state depending on initial conditions. On the other hand, when kin competition is high (low K) the additional pressure to reduce dispersal due to the introduction of specialization is counteracted by the drive to disperse to avoid competition with kin. Thus the feedback loop is mediated by the level of kin competition, and in this low K case, the drop in dispersal and increase in variance of local adaptation will be much smaller. This result also holds for asymmetrical environments, which we have explored numerically.

In our model, the distribution of site types is smooth, with a single peak, however if branching in ecological character has occurred, the distribution of x is banded, with multiple, evenly spaced, peaks. Thus competitive exclusion, though not explicitly included in our model, emerges from the dynamics and there is a limit to the similarity between co-existing branches (Meszéna et al., 2006), which depends on the level of population structure. We do not have a satisfactory explanation for the mechanisms behind the observed competitive exclusion or why the apparent niche overlap (May, 1974) decreases with decreased kin competition (increased K). This is an area for further analytic work.

The present model is similar in spirit to that of Nurmi and Parvinen (2011) who also modeled the joint evolution of dispersal and specialization in a metapopulation context; however, the details of specialization and the pressures controlling the level of dispersal were quite different. Unlike Nurmi and Parvinen (2011) we did not see the co-existence of high and low dispersers (except in a small region, just above σ_c). However, they observed this evolutionary outcome when they had three distinct patch types, rather than a continuum as we had. If we had three, evenly spaced, patch types in our model, such that a specialist on the rightmost would be viable only on the right and middle type patches, and the specialist on the leftmost only viable on the left and middle, then we would expect a generalist type, which would be viable all three, to have a higher dispersal that the two specialist. Thus our continuum-based approach suggests that the dimorphism in dispersal may be due to the discrete site types they used. Kisdi (2002) also observed this coexistence, but again using a model with two discrete patch types.

Our results are consistent with the comparable case (asexual reproduction and wide competition amongst individuals with different ecological types) of Heinz et al. (2009) who used a similar, but spatially explicit model. Our

analysis matches the sharp transition they found between regions of selection for highly dispersing generalists and more sedentary specialists, and shows how it is mediated by environmental heterogeneity and local kin competition. When sexual reproduction is introduced into their model this boundary is smoother, and there is an intermediate zone of short range dispersal but no specialization. Thus it would be interesting to know if sexual reproduction would eliminate such a transition in general. Potentially the discrete spacial structure of our model would prevent this as would the addition of assortative mating.

Potentially shedding light on that question, Billiard and Lenormand (2005) and Blanquart and Gandon (2014) indeed observed a sharp cut-off between regions of high and low dispersal in genetically explicit models with sexual reproduction. In these models dispersal probability could evolve continuously, but the gene controlling it was on the same chromosome as a local adaptation gene, which did not evolve, but was under differential spatial selection. Both Billiard and Lenormand (2005) (using a two patch model) and Blanquart and Gandon (2014) (using a metapopulation model) found three distinct parameter regions: one selecting for a highly dispersing population, which was monomophic in the specialization trait, another selecting for a rarely dispersing population with a protected polymorphism in the specialization trait, and finally a region between the other two regions where either of the preceding two populations could be selected for, depending on the initial conditions. This is analogous to the right panel of our Figure 5 and led to hysteresis in their models. This suggests that the sharp boundary and discontinuities could be preserved under sexual reproduction. However, there was no feedback in these models because specialization could not evolve, only be maintained or lost. Thus the discontinuities in dispersal were likely due to the binary nature of the specialization trait and the question of joint evolution of dispersal and local adaptation leading to sharp transitions as in Heinz et al. (2009) and the present study, under sexual reproduction, is still open.

Day (2001) investigated the role of dispersal and population structure on the evolution of local adaptation using a similar metapopulation model with some key differences. While both studies characterize environmental variation using a normal distribution, Day's model has within site variance of habitat type but zero variance between sites, while we have zero variance within a site but variance between sites. This difference leads to an opposite trend between dispersal and local adaptation. In Day's scenario, low dispersal means that mutants that vary in their ecological character come back and compete (less) with one another, thus selecting for branching in the ecological trait, while in our model, low dispersal means a lineage will experience less variation in habitat trait and thus can more easily specialize.

More recently, Svardal et al. (2015) explored how dispersal and temporal environmental heterogeneity drive adaptive radiation in a local adaptation parameter. Their analytic results are in qualitative agreement with our generalist-specialist boundary (v_c), however, dispersal is fixed in their model so there is no feedback between dispersal and

local-adaptation. Concentrating on temporal heterogeneity in the environment they are able to show how changing the sign of the auto-correlation (positive or negative) in the environmental condition at a site switches the trend in the threshold value of dispersal, below which one would expect branching to occur.

The existence of critical thresholds in evolutionary outcomes is important for our ecological understanding but may also have ramifications for conservation. Many anthropogenic changes such as development, urbanization or agriculture tend to homogenize environments and ecosystems. Climate change is another factor that could alter environmental heterogeneity in either direction. The eco-evolutionary implications of our results show that such changes can shift a population of low-dispersing specialists to highly dispersing generalists, or vice versa. Further, habitat degradation or the introduction of an invasive species that increases predation or competition may reduce the effective carrying capacity of an environment which could shift populations in an analogous way. Likewise, changes in harvesting or management regimes, such as a reduction in the escapement of spawning salmon, could trigger a similar transition and have non-linear effects on several ecosystem variables that would be unexpected based on a traditional stock management model. Further, because our model exhibits hysteresis between the two regimes, once a system is perturbed beyond this threshold in any of these ways, it may not return to its original state even after the perturbation has subsided.

Since our model is very general it may be applicable (in a qualitative sense) to many scenarios in nature. Our evolution of a probability to disperse, or not, is analogous to the evolution of a characteristic dispersal distance greater than, or less than, the correlation length of the ecological trait in the environment in a spatial model. We assume no energetic or morphological cost of dispersal (only the risk of ending up on ill-suiting habitat). This assumption is fitting for many species of migratory breeders, in taxa as diverse as fish, birds, ungulates and insects, where all breeding adults must pay the energetic cost to migrate to breeding grounds (Schtickzelle and Quinn, 2007). For example, adult pacific salmon migrate from the sea to discrete freshwater breeding streams but may either home to their natal stream or stray to a novel site, making them well suited to a metapopulation approach (Schtickzelle and Quinn, 2007). Further, these fish are known to be strongly locally adapted to streams with specific continuous conditions such as temperature, water depth or substrate size (Fraser et al., 2011; Hendry et al., 2000; Peterson et al., 2014; Westley et al., 2013).

The simplicity of our model makes it well suited for expansion and adaptation. Possible extensions include a cost of (or probability to perish during) dispersal, stochastic local extinctions, and other functional forms for the distribution of site types, $p(x)$, all of which should fit into our analytical framework. Additionally, for adaptation to certain environmental features, competition between individuals could be stronger when their ecological traits are more similar, and this could be incorporated as in Heinz et al. (2009). Relaxing the assumption of a constant carrying

capacity across sites may lead to interesting results (Massol et al., 2011), as would modifying the order of events in the model life-cycle to reflect alternate life histories and selection regimes (Débarre and Gandon, 2011; Johst and Brandl, 1997; Massol, 2013; Ravigné et al., 2004). Further, our model is asexual and phenotype-based. This approach may be directly relevant to competition between different species, but can also have analogues for populations of a single sexually reproducing species. However, modelling a similar situation with sexual reproduction and explicit genetic architecture and dynamics (Billiard and Lenormand, 2005; Blanquart and Gandon, 2014; North et al., 2011) may well lead to further interesting results. Finally, dispersal can be the result of errors in navigation during breeding migrations, leading errant individuals to breed at non-natal sites. Navigational ability can be socially facilitated (Mueller et al., 2013), or density dependent (Berdahl et al., 2013, 2014), thus incorporating collective effects such as herding, flocking or schooling, which are common in many migratory species, into models of dispersal is an exciting avenue for further work in this area.

7. ACKNOWLEDGEMENTS

We are grateful to Éva Kisdi, and two anonymous referees for suggesting substantial improvements to our analysis and this manuscript. We would also like to thank Iain Couzin, Orion Penner and Vishal Sood for insightful discussions and Bill Wichser and Robert Knight for computing support. Simulations were performed using Princeton University's Tiger cluster. This work was supported by the Natural Sciences and Engineering Research Council of Canada, the Yukon Foundation, and the Army Research Office Grant No. W911NG-11-1-0385.

8. REFERENCES

Ajar, É. (2003). Analysis of disruptive selection in subdivided populations. *BMC evolutionary biology*, 3(1):22.

Bengtsson, B. (1978). Avoiding inbreeding: at what cost? *J. Theor. Biol.*, 73:439–444.

Berdahl, A., Torney, C. J., Ioannou, C. C., Faria, J. J., and Couzin, I. D. (2013). Emergent sensing of complex environments by mobile animal groups. *Science*, 339:574–576.

Berdahl, A., Westley, P. A., Levin, S. A., Couzin, I. D., and Quinn, T. P. (2014). A collective navigation hypothesis for homeward migration in anadromous salmonids. *Fish Fish.*

Billiard, S. and Lenormand, T. (2005). Evolution of migration under kin selection and local adaptation. *Evolution*, 59:13–23.

Blanquart, F. and Gandon, S. (2011). Evolution of migration in a periodically changing environment. *The Am. Nat.*, 177(2):188–201.

Blanquart, F. and Gandon, S. (2014). On the evolution of migration in heterogeneous environments. *Evolution*, 68(6):1617–1628.

Chaianunporn, T. and Hovestadt, T. (2012). Concurrent evolution of random dispersal and habitat niche width in host-parasitoid systems. *Ecol. Modell.*, 247:241–250.

Chesson, P. L. (1984). Persistence of a markovian population in a patchy environment. *Zeitschrift für Wahrscheinlichkeitstheorie und Verwandte Gebiete*, 66(1):97–107.

Cohen, D. and Levin, S. A. (1987). The interaction between dispersal and dormancy strategies in varying and heterogeneous environments. In *Mathematical Topics in Population Biology, Morphogenesis and Neurosciences*, pages 110–122. Springer.

Cohen, D. and Levin, S. A. (1991). Dispersal in patchy environments: the effects of temporal and spatial structure. *Theor. Popul. Biol.*, 39:63–99.

Colbert, J., Danchin, E., Dhondt, A., and Nichols, J. (2001). *Dispersal*. Oxford University Press, New York.

Comins, H., Hamilton, W., and May, R. (1980). Evolutionarily stable dispersal strategies. *J. Theor. Biol.*, 82:205–230.

Coyne, J. A., Orr, H. A., et al. (2004). *Speciation*. Sinauer Associates Sunderland, MA.

Crowley, P. H. and McLetchie, D. N. (2002). Trade-offs and spatial life-history strategies in classical metapopulations. *Am. Nat.*, 159:190–208.

Day, T. (2001). Population structure inhibits evolutionary diversification under competition for resources. *Genetica*, 112-113:71–86.

Débarre, F. and Gandon, S. (2011). Evolution in heterogeneous environments: between soft and hard selection. *Am. Nat.*, 177(3):E84–E97.

Doebeli, M. and Dieckmann, U. (2003). Speciation along environmental gradients. *Nature*, 421:259–264.

Duputié, A. and Massol, F. (2013). An empiricist's guide to theoretical predictions on the evolution of dispersal. *Interface focus*, 3(6):20130028.

Dytham, C. and Travis, J. J. M. (2006). Evolving dispersal and age at death. *Oikos*, 113:530–538.

Fraser, D. J., Weir, L. K., Bernatchez, L., Hansen, M. M., and Taylor, E. B. (2011). Extent and scale of local adaptation in salmonid fishes: review and meta-analysis. *Heredity*, 106(3):404–420.

Futuyma, D. J. and Moreno, G. (1988). The evolution of ecological specialization. *Annu. Rev. Ecol. Syst.*, 19:207–233.

Gandon, S. (1999). Kin competition, the cost of inbreeding and the evolution of dispersal. *J. Theor. Biol.*, 200:345–364.

Geritz, S. A., Kisdi, É., Mesze, G., and Metz, J. (1998). Evolutionarily singular strategies and the adaptive growth and branching of the evolutionary tree. *Evol. Ecol.*, 12(1):35–57.

Geritz, S. A., van der Meijden, E., and Metz, J. A. (1999). Evolutionary dynamics of seed size and seedling competitive ability. *Theor. Popul. Biol.*, 55(3):324–343.

Guillaume, F. and Perrin, N. (2006). Joint evolution of dispersal and inbreeding load. *Genetics*, 173:497–509.

Hamilton, W. and May, R. (1977). Dispersal in stable habitats. *Nature*, 269:578–581.

Hastings, A. (1983). Can spatial variation alone lead to selection for dispersal? *Theor. Popul .Biol.*, 24:244–251.

Heinz, S., Mazzucco, R., and Dieckmann, U. (2009). Speciation and the evolution of dispersal along environmental gradients. *Evol. Ecol.*, 23:53–70.

Hendry, A. P., Wenburg, J. K., Bentzen, P., Volk, E. C., and Quinn, T. P. (2000). Rapid evolution of reproductive isolation in the wild: evidence from introduced salmon. *Science*, 290:516–518.

Holt, R. D. (1985). Population dynamics in two-patch environments: some anomalous consequences of an optimal habitat distribution. *Theor. Popul. Biol.*, 28(2):181–208.

Ito, H. C. and Dieckmann, U. (2007). A new mechanism for recurrent adaptive radiations. *Am. Nat.*, 170:E96–E111.

Johnson, M. L. and Gaines, M. S. (1990). Evolution of dispersal: theoretical models and empirical tests using birds and mammals. *Annu. Rev. Ecol. Syst.*, 21:449–480.

Johst, K. and Brandl, R. (1997). Evolution of dispersal: the importance of the temporal order of reproduction and dispersal. *Proc. R. Soc. B*, 264(1378):23–30.

Kisdi, É. (2002). Dispersal: Risk spreading versus local adaptation. *Am. Nat.*, 159:579–596.

Le Galliard, J.-F., Ferriere, R., and Dieckmann, U. (2005). Adaptive evolution of social traits: origin, trajectories, and correlations of altruism and mobility. *Am. Nat.*, 165:206–224.

Lehmann, L. and Perrin, N. (2003). Inbreeding avoidance through kin recognition: choosy females boost male dispersal. *Am. Nat.*, 162:638–652.

Leimar, O. (2005). The evolution of phenotypic polymorphism: randomized strategies versus evolutionary branching. *Am. Nat.*, 165:669–681.

Leturque, H. and Rousset, F. (2002). Dispersal, kin competition, and the ideal free distribution in a spatially heterogeneous population. *Theor. Popul .Biol.*, 62:169–180.

Leturque, H. and Rousset, F. (2003). Joint evolution of sex ratio and dispersal: conditions for higher dispersal rates from good habitats. *Evol. Ecol.*, 17:67–84.

Levin, S. A., Cohen, D., and Hastings, A. (1984). Dispersal strategies in patchy environments. *Theor. Popul. Biol.*, 26(2):165 – 191.

Levin, S. A., Muller-Landau, H. C., Nathan, R., and Chave, J. (2003). The ecology and evolution of seed dispersal: a theoretical perspective. *Annu. Rev. Ecol. Evol. Syst.*, pages 575–604.

Ludwig, D. and Levin, S. A. (1991). Evolutionary stability of plant communities and the maintenance of multiple dispersal types. *Theor. Popul. Biol.*, 40:285–307. Erratum: (42)104–105.

Massol, F. (2013). A framework to compare theoretical predictions on trait evolution in temporally varying environments under different life cycles. *Ecol. Complex.*, 16:9–19.

Massol, F. and Cheptou, P.-O. (2011). Evolutionary syndromes linking dispersal and mating system: the effect of autocorrelation in pollination conditions. *Evolution*, 65(2):591–598.

Massol, F., Duputié, A., David, P., and Jarne, P. (2011). Asymmetric patch size distribution leads to disruptive selection on dispersal. *Evolution*, 65:490–500.

May, R. M. (1974). On the theory of niche overlap. *Theor. Popul. Biol.*, 5(3):297–332.

Maynard Smith, J. and Price, G. (1973). The logic of animal conflict. *Nature*, 246:15.

Meszéna, G., Gyllenberg, M., Pásztor, L., and Metz, J. A. (2006). Competitive exclusion and limiting similarity: a unified theory. *Theor. Popul. Biol.*, 69(1):68–87.

Metz, J. and Gyllenberg, M. (2001). How should we define fitness in structured metapopulation models? including an application to the calculation of evolutionarily stable dispersal strategies. *Proc. R. Soc. Lond. B Biol. Sci.*, 268:499–508.

Metz, J., Nisbet, R., and Geritz, S. (1992). How should we define fitness for general ecological scenarios? *Trends Ecol. Evol.*, 7(6):198–202.

Mueller, T., OHara, R. B., Converse, S. J., Urbanek, R. P., and Fagan, W. F. (2013). Social learning of migratory performance. *Science*, 341(6149):999–1002.

North, A., Pennanen, J., Ovaskainen, O., and Laine, A.-L. (2011). Local adaptation in a changing world: The roles of gene-flow, mutation, and

sexual reproduction. *Evolution*, 65:79–89.

Nurmi, T. and Parvinen, K. (2011). Joint evolution of specialization and dispersal in structured metapopulations. *J. Theor. Biol.*, 275:78–92.

Olivieri, I. (2001). The evolution of seed heteromorphism in a metapopulation: interactions between dispersal and dormancy. *Integrating ecology and evolution in a spatial context*, pages 245–266.

Parvinen, K. (2013). Joint evolution of altruistic cooperation and dispersal in a metapopulation of small local populations. *Theor. Popul .Biol.*, 85:12–19.

Perrin, N. and Mazalov, V. (2000). Local competition, inbreeding, and the evolution of sex-biased dispersal. *Am. Nat.*, 155:116–127.

Peterson, D. A., Hilborn, R., and Hauser, L. (2014). Local adaptation limits lifetime reproductive success of dispersers in a wild salmon metapopulation. *Nat. Commun.*, 5.

Pusey, A. and Wolf, M. (1996). Inbreeding avoidance in animals. *Trends Ecol. Evol.*, 11:201–206.

Ravigné, V., Olivieri, I., Dieckmann, U., et al. (2004). Implications of habitat choice for protected polymorphisms. *Evol. Ecol. Res.*, 6(1):125–145.

Ravigné, V., Olivieri, I., Martinez, S. G., and Rousset, F. (2006). Selective interactions between short-distance pollen and seed dispersal in self-compatible species. *Evolution*, 60:2257–2271.

Ronce, O. (2007). How does it feel to be like a rolling stone? ten questions about dispersal evolution. *Annu. Rev. Ecol. Evol. Syst.*, 38:231–253.

Ronce, O., Perret, F., and Olivieri, I. (2000). Landscape dynamics and evolution of colonizer syndromes: interactions between reproductive effortand dispersal in a metapopulation. *Evol. Ecol.*, 14:233–260.

Schluter, D. (2000). *The ecology of adaptive radiation.* Oxford University Press, USA.

Schtickzelle, N. and Quinn, T. P. (2007). A metapopulation perspective for salmon and other anadromous fish. *Fish Fish.*, 8:297–314.

Svardal, H., Rueffler, C., and Hermisson, J. (2015). A general condition for adaptive genetic polymorphism in temporally and spatially heterogeneous environments. *Theor. Popul. Biol.*, 99:76–97.

Turelli, M., Barton, N. H., and Coyne, J. A. (2001). Theory and speciation. *Trends Ecol. Evol.*, 16:330–343.

Venable, D. L. and Brown, J. S. (1988). The selective interactions of dispersal, dormancy, and seed size as adaptations for reducing risk in variable environments. *Am. Nat.*, 131:360–384.

Westley, P. A., Ward, E. J., and Fleming, I. A. (2013). Fine-scale local adaptation in an invasive freshwater fish has evolved in contemporary time. *Proc. R. Soc. Lond. B Biol. Sci.*, 280.

Table 1: Overview of notation.

Label	Description
v	Probability to disperse, prime denotes rare invader Evolvable, restricted to $0 \leq v \leq 1$
x	Ecological character, prime denotes rare invader Evolvable, unrestricted
x^*, v^*	Evolutionary singular strategies calculated for monomorphic populations
$\tilde{v}$	Evolutionary and convergence stable dispersal rate for monomorphic or polymorphic populations
z	Ecological type of a site
$p(z)$	Distribution of ecological site types (equation 1)
L	Number of sites in metapopulation (set to $8192/K$ for simulations)
K	Carrying capacity at each site
σ	Environmental heterogeneity: σ_z/σ_m
σ_z	Width of site type distribution, $p(z)$
σ_m	Width of fecundity curve (set to 1 for simulations)
m_0	Maximum fecundity (set to 128 for simulations)
$m(x,z)$	Fecundity of individual with ecological character x on site of type z (equation 2)
$\bar{m}(x)$	Average number of offspring produced, per site, by a resident of type x, over all sites
$M(z)$	Expected number of offspring a mutant lineage will produce before losing a site of type z
R_m	Metapopulation reproduction ratio

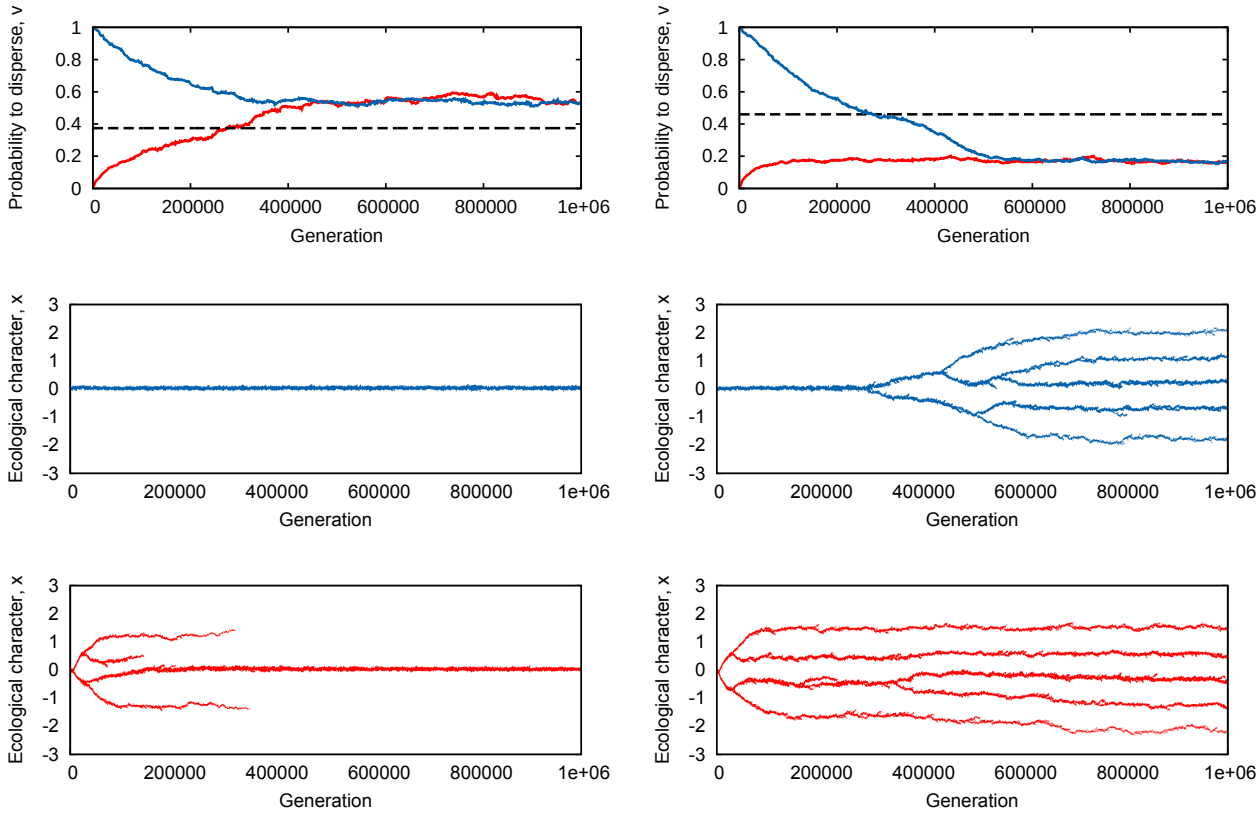

Figure 1: Evolutionary trajectories of dispersal probability and ecological character over time. The left and right columns are for environmental heterogeneity of 0.75 and 0.90 respectively. Top row of panels: Evolution of the mean probability to disperse as a function of time (generation). The blue curves are for simulations starting with full dispersal ($v = 1$), while the red curves are for simulations starting with no dispersal ($v = 0$). The dashed black line shows the threshold level of v, below which branching in x will occur for that specific value of environmental heterogeneity (this is v_c, the generalist-specialist boundary shown in Figure 2). Middle and lower panels: The evolution of the ecological trait, x, as a function of time; each vertical slice represents the distribution of x in the population at that time. The middle panels correspond to the blue curves in the top panels, that is those simulations begin with $v = 1$. The lower panels correspond to the red curves in the top panels; those simulations begin with $v = 0$. For lower environmental heterogeneity (left panels; $\sigma = 0.75$) branching in x occurs when the population starts with no dispersal, but these specialist branches are replaced by a monomorphic generalist population with having $x = 0$ when v crosses the threshold denoted by the dashed black line. Conversely, for higher environmental heterogeneity (right panels; $\sigma = 0.90$), if starting with full dispersal, branching in x does not occur until v falls below the threshold value. All data are for $K = 8$.

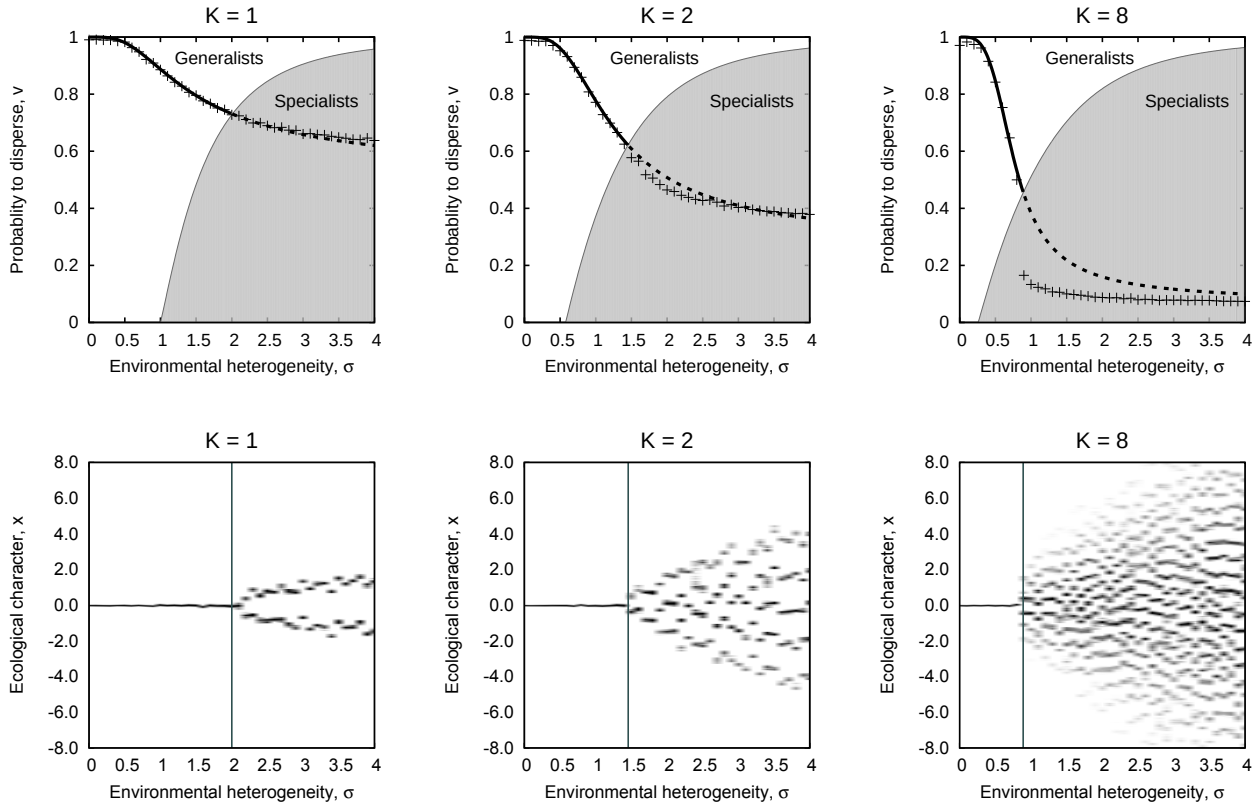

Figure 2: Joint evolution of dispersal probability and ecological character as a function of environmental heterogeneity. Top panels: Probability to disperse, v, as a function of environmental heterogeneity, σ. The black line shows the stationary strategy, v^*, given by the solution to Equation 7; where it is solid the strategy is evolutionarily stable and where it is broken the strategy is not evolutionarily stable. The crosses depict the evolved value of v from numerical simulations averaged over the population (initial conditions: monomorphic population with $v = 1$, $x = 0$). The white and gray areas show, for fixed values of dispersal and environmental heterogeneity, whether the evolution will select for generalists or specialist, respectively - i.e. whether or not the singular strategy at $x^* = 0$ is evolutionarily stable (negative definite Hessian). The thin grey line separating the white and grey regions shows v_c, the threshold value of dispersal for a given σ and K. For large K ($K = 8$ shown here) a discontinuity in $\tilde{v}$ occurs as the $x^* = 0$ strategy becomes unstable and the population shifts from generalists to specialists. Bottom panels: Distribution of evolved ecological character, x, as a function of environmental heterogeneity. Each vertical slice represents the probability distribution of x for that value of the environmental heterogeneity. The $x^* = 0$ strategy becomes unstable at a critical value of environmental heterogeneity, σ_c, and branching occurs. This threshold value corresponds to the point at which the v^* curve passes over the boundary between selection for generalists and specialists - i.e. when $v^* = v_c$. The vertical line depicts the theoretical value of σ_c. As environmental heterogeneity is increased beyond this threshold the number of discrete specialist types increases. The vertical pairs of panels from left to right are for $K = 1$, $K = 2$ and $K = 8$.

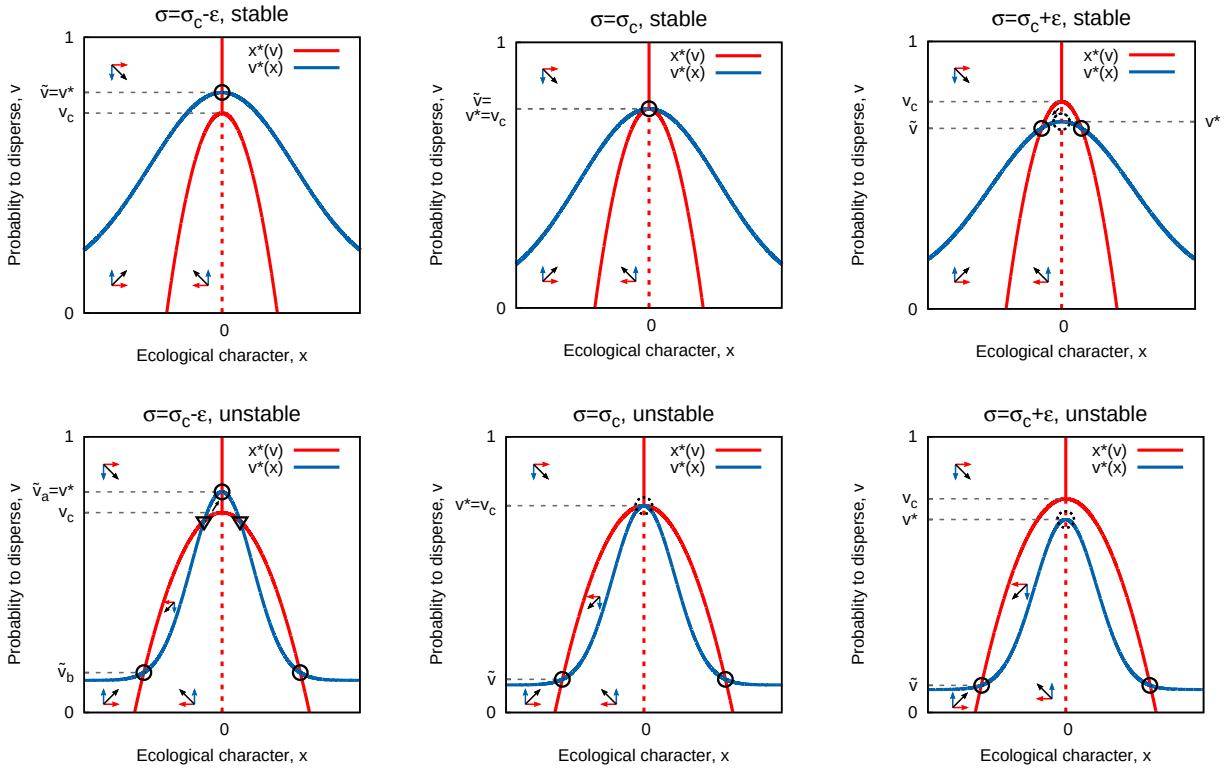

Figure 3: Schematic diagrams explaining the discontinuity and hysteresis in the evolved probability to disperse. We consider a dimorphic population, half having ecological character x and the other half having $-x$ all of which have the same probability to disperse, v. The red and blue curves correspond to the nullclines of the evolutionary gradient for this dimorphic, symmetric population in v-x space. The value of v where the red curve, $\pm x(v)$, splits from $x = 0$ is v_c, the boundary that separates the generalist and specialist regions of Figure 2. The peak of the blue curve, $v(x = 0)$, is v^*, the solution to Equation 7 (black line in Figure 2). The evolutionary dynamics will tend, in the vertical direction, towards the blue line and, in the horizontal direction, towards to the red curve. Arrows with the corresponding colors show the general direction of evolution in each section of the diagram (sum in black). Intersections of solid blue and red curves correspond to singular strategies, which can be ESSs (solid black circles) or divergent (dashed black circles) depending on the relative slope at the intersection. If the red line is dashed the dynamics will be divergent and thus the singular strategy is not stable. In each row environmental heterogeneity, σ, increased from left to right, which tends to increase v_c and decrease v^*. They are equal in the middle panels ($\sigma = \sigma_c$).

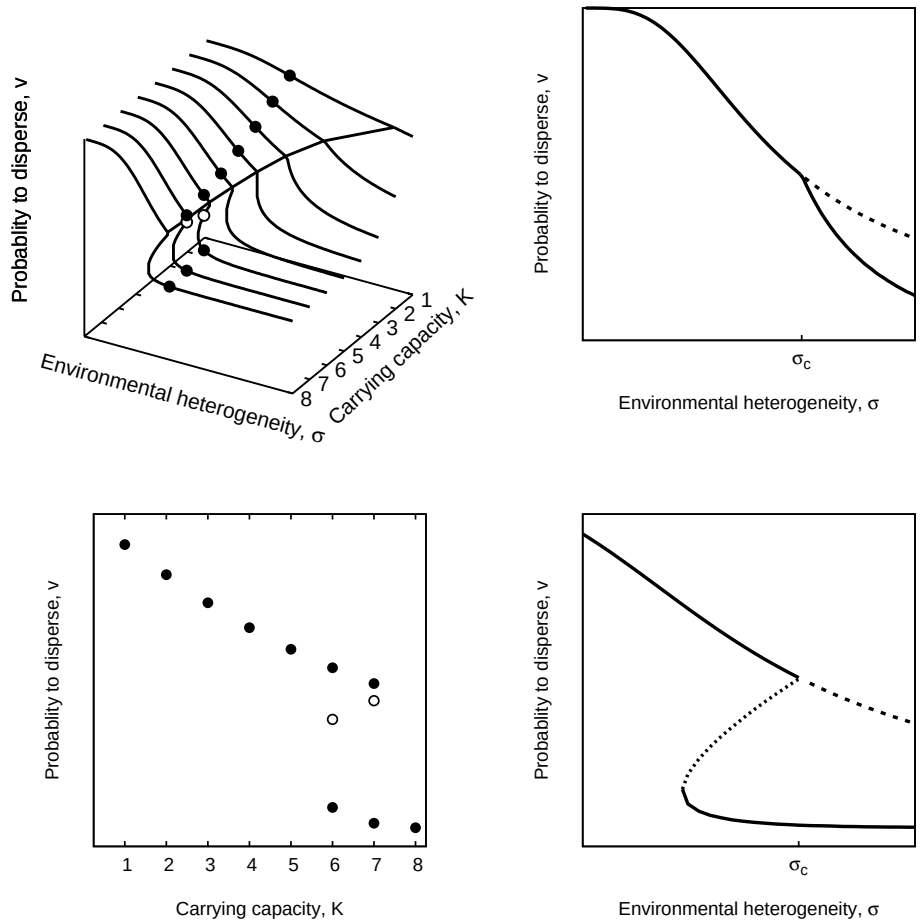

Figure 4: Schematic of the ESS dispersal probability, $\tilde{v}$, from the dimorphic invasion plots (Figures 3 and F.4) as a function of environmental heterogeneity and carrying capacity. Top left panel: the joint evolution of dispersal and local adaptation leads to a bifurcation in the evolved probability to disperse. Right panels: $\tilde{v}$ as a function of σ for a fixed K (single slice of 3D plot), the top panel shows $K = 2$ and the bottom $K = 8$. The top and bottom right panels correspond to the top and bottom row of Figure 3 respectively. Solid lines indicate ESSs and correspond to solid circles in Figure 3. Dashed lines indicate convergence, but not evolutionary stable strategies (the instability occurring in the other trait) – dashed circles in Figure 3. Dotted lines represent unstable singular strategies corresponding to the triangles in Figure 3. In the top solid line the population will all have $x = 0$ while in the lower sold line the population will be dimorphic, half with x and the other half $-x$. Bottom left: $\tilde{v}$ as a function of carrying capacity, K. There is potential for bistability and hysteresis as a function of K for some values of σ. Filled circles are stable, empty unstable. These points are also shown on the 3D plot.

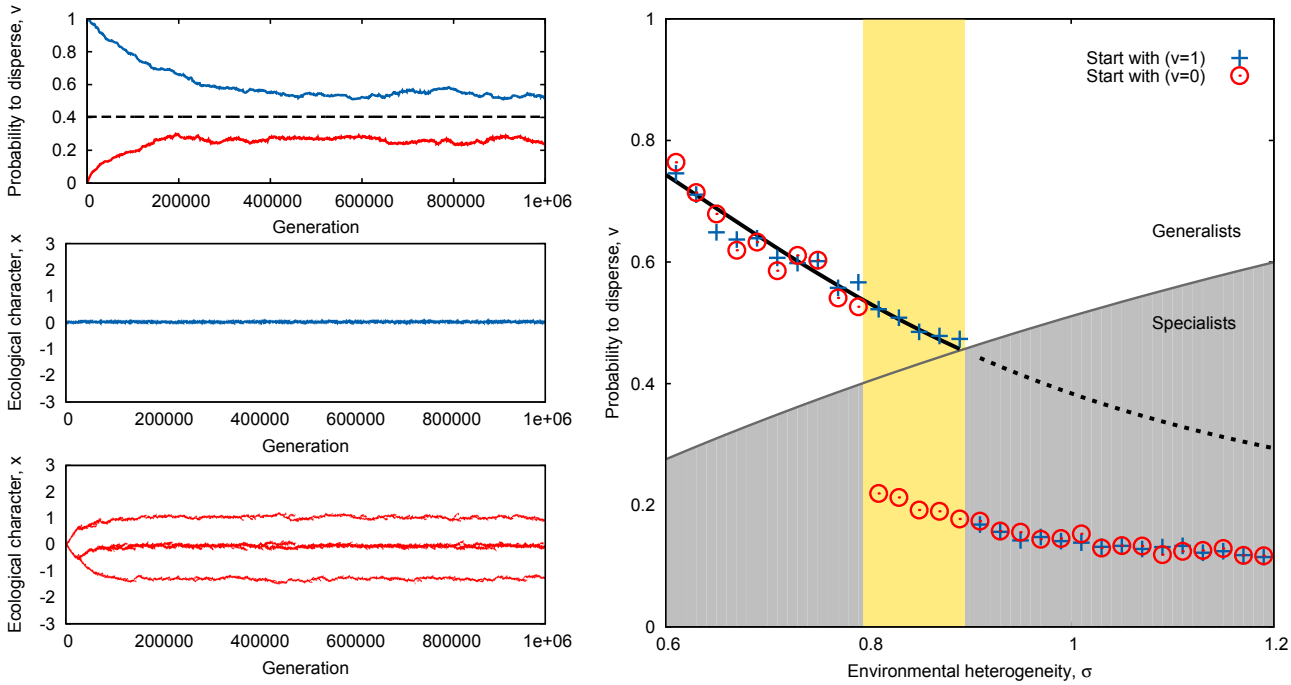

Figure 5: Bistability and hysteresis. The left panels, details as in Figure 1, show that for values of σ slightly below σ_c (σ = 0.8 shown here) the population can alternately exist in the highly dispersing generalist, or the rarely dispersing specialist state depending on the initial condition of the simulation, here starting with full (middle panel) or no (bottom panel) dispersal. The right panel, details as in Figure 2, shows the extent of this region of bistability (shaded yellow region), and illustrates how the discontinuities in mean evolved v and the variance of x due to the evolutionary feedback between dispersal and local adaptation lead to a hysteresis loop. Blue crosses indicate numerical runs starting with highly dispersing generalists (v = 1, x = 0) and red circles are for runs starting with rarely dispersing specialists (v = 0, x = z). Note, some simulations in the yellow region, starting with sedentary specialists, did reach the upper equilibrium (not shown). All data for K = 8.